Supporting Information

Lee et al. 10.1073/pnas.1314427110

SI Materials and Methods

Brain Slice Preparation and Electrophysiology. Transverse brainstem slices (200 μm thick) containing the medial nucleus of trapezoid body were prepared from Sprague–Dawley rats. Protocols were approved by the Animal Care Committee of Seoul National University. The brains obtained from 7- to 9-d-old rats were chilled in ice-cold low-calcium artificial cerebrospinal fluid (aCSF). Slices were made using a Vibratome slicer (VT1200; Leica) and incubated at 37 °C for 30 min in normal aCSF and thereafter maintained at room temperature (23–25 °C) until required. Low-calcium aCSF contained (in mM) 125 NaCl, 25 $NaHCO_3$, 2.5 KCl, 1.25 NaH_2PO_4, 2.5 $MgCl_2$, 0.5 $CaCl_2$, 25 glucose, 0.4 Na ascorbate, 3 myoinositol, and 2 Na pyruvate [pH 7.4 when saturated with carbogen (95% O_2, 5% CO_2); osmolarity, ~320 mOsm]. The constituents of normal aCSF are the same as low-calcium aCSF except with 1 mM $MgCl_2$ and 2 mM $CaCl_2$. Slices were transferred to a recording chamber in an upright microscope (BX50WI; Olympus). In most experiments, 1 μM tetrodotoxin, 50 μM D-AP5, and 10 mM TEA-Cl were added to the normal aCSF to isolate presynaptic Ca^{2+} current and AMPA receptor-mediated excitatory postsynaptic currents (EPSCs). Moreover, 100 μM cyclothiazide and 2 mM γ-D-glutamylglycine (γ-DGG; low-affinity AMPA receptor antagonist) were added to prevent desensitization and saturation of AMPA receptors, respectively. A total of 2 mM γ-DGG reduced the EPSC amplitude to one half of the control value. A presynaptic terminal and the postsynaptic MNTB neurons were simultaneously whole-cell patch-clamped at −80 mV and −70 mV, respectively. The postsynaptic pipette (2–3 MΩ) solution contained (in mM) 130 Cs-gluconate, 20 TEA-Cl, 10 NaCl, 20 Hepes, 5, Na-phosphocreatine, 4 Mg-ATP, and 10 EGTA, pH adjusted at 7.3. The presynaptic patch pipette (3–4 MΩ) solution contained (in mM) 130 Cs-gluconate, 20 TEA-Cl, 20 Hepes, 5 Na-phosphocreatine, 4 Mg-ATP, 0.3 Na-GTP, and 0.5 EGTA, with pH adjusted at 7.3 using CsOH. The presynaptic series resistance (R_S, 10–25 MΩ) was compensated by 50% to 80%, and the postsynaptic R_S (4–15 MΩ) was compensated by as much as 70%, such that remaining uncompensated R_S values were 5 MΩ and 3 to 4 MΩ for pre- and postsynaptic pipettes, respectively. The remaining postsynaptic resistance was further compensated off-line. To obtain square-like presynaptic calcium currents, predepleting pulses (preDPs) or depleting pulses (DPs) were comprised of depolarization to 0 mV preceded by predepolarizations to +70 mV for 2 ms. The duration of preDP or DP is defined by the duration of the 0 mV step. The whole-cell recordings were made by using an EPC10/2 amplifier (HEKA) at room temperature. TTX, DL-AP5, cyclothiazide, and γ-DGG were purchased from Tocris. Calmodulin inhibitory peptide, latrunculin B, calmidazolium, U73122, U73343, and edelfosine were obtained from Calbiochem. All other chemicals were obtained from Sigma. Lipid-soluble drugs were dissolved with a final DMSO concentration of 1/1,000 (vol/vol). The same DMSO was added under control conditions. We confirmed that these drugs have little effect on baseline parameters of EPSCs compared with their vehicle (DMSO).

Deconvolution Method. Quantal release rates were estimated by using a deconvolution method, which also corrects for delayed glutamate clearance from the synaptic cleft at the calyx of Held synapse (ref. 1; see also www.mpibpc.mpg.de/groups/neher). By using the so-called "fitting protocol," we determined parameters of the glutamate diffusion model, which is embedded in the deconvolution routine at the start of each experiment. The criteria for an appropriate parameter set were described previously (2). After determining the parameters for a given synapse, we used the same parameters for all traces within a given cell pair. Cumulative release was calculated by the integration of release rate traces after correction of vesicle replenishment by using the calcpool routine (3), and fitted with a biexponential function. We applied the correction of refilling only for the quantal release induced by 30-ms depolarizations, assuming a refilling time constant of 0.5 s (4). The fits extended from the onset of release to 10 to 20 ms after the end of stimulation. The sizes and the release time constants of two vesicle pools [fast-releasing pools (FRPs) and slowly releasing pools (SRPs)] were obtained from the fitting, with the FRP being taken as the faster component of the biexponential fit. In the dual-pulse protocol, the response to the second stimulus was also fitted with a biexponential function, allowing for two time constants as free parameters. Restriction of the time constants to the values of fits to the conditioning episodes did not result in satisfactory fits, especially when the fast component was not fully recovered at a short interstimulus interval (ISI) after a preDP of 3 ms (preDP3) or 10 ms (preDP10).

Data Analysis. Data were analyzed by using IgorPro (version 6.0; WaveMetrics). Statistical data are expressed as mean ± SEM, and n indicates the number of synapses studied. Statistical analyses on data obtained from the same synapse and those on data from different synapses were performed by using a Student paired t test and the Student t test, respectively. Statistical significance was determined with a threshold P value of 0.05 or 0.01. For simplicity, some statistical data with no significant difference are not shown in the text.

SI Discussion

Fig. 5 compares the time courses of the fast time constant (τ_{fast}) recovery after a preDP3 or a preDP10 under control conditions and in the presence of 1-oleoyl-2-acetyl-sn-glycerol (OAG). Under control conditions, the time courses after these two preDPs were not different. In the presence of OAG, however, τ_{fast} was accelerated already at the shortest ISI (200 ms) after a preDP3, whereas the OAG effect became apparent after a preDP10 only at an ISI of 2 s. Why does the effect of OAG on τ_{fast} recovery become evident earlier for synaptic vesicles (SVs) recruited via SRP-dependent recovery compared with those recovered after a preDP10? This difference in the OAG effect between preDP3 and preDP10 may be explained by assuming that time is required for an SV that just attained fusion competence to be "superprimed," even under conditions of sufficient supply of OAG. Under this assumption, SVs recruited via SRP-dependent recovery after a preDP3 in the presence of OAG may be already more advanced in molecular priming because their release apparatus had been exposed to high [OAG] for appreciable time before being recruited to the FRP. On the contrary, SVs recruited after a preDP10 would all be derived from the recycling pool and would form their release apparatus only after the preDP10, such that OAG cannot act on them until they attain fusion competence. Recovery of the FRP size after a preDP10 was minimal and was not affected by latrunculin B, indicating that it represents a basal recovery rate independent of residual SRP. It is not clear whether FRP vesicles after a preDP10 are recruited directly from a recycling pool or through an intermediate SRP stage (or both). Assuming that the FRP is

recovered directly by recruitment of SVs from a recycling pool after a preDP10, the latency may represent the time required for Munc13s to superprime the SVs that have just attained fusion competence. Taken together, the differential effect of OAG after a preDP3 and preDP10 is consistent with the idea that SVs recruited after a preDP3 are already release-competent but need a last step to be fully matured, whereas the FRP recovery after a preDP10 may involve recruitment of SVs from a recycling pool.

1. Neher E, Sakaba T (2001) Combining deconvolution and noise analysis for the estimation of transmitter release rates at the calyx of held. *J Neurosci* 21(2):444–461.
2. Lee JS, Ho WK, Lee SH (2012) Actin-dependent rapid recruitment of reluctant synaptic vesicles into a fast-releasing vesicle pool. *Proc Natl Acad Sci USA* 109(13): E765–E774.
3. Sakaba T, Neher E (2001) Quantitative relationship between transmitter release and calcium current at the calyx of held synapse. *J Neurosci* 21(2):462–476.
4. Hosoi N, Sakaba T, Neher E (2007) Quantitative analysis of calcium-dependent vesicle recruitment and its functional role at the calyx of Held synapse. *J Neurosci* 27(52): 14286–14298.

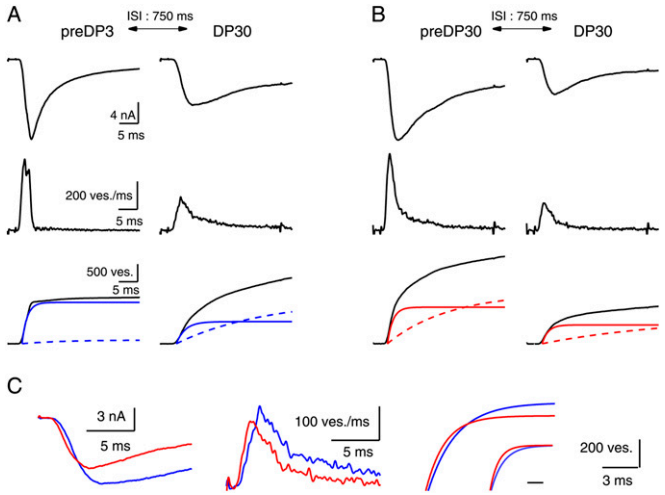

Fig. S1. Representative traces for EPSCs, quantal release rates, and cumulative release evoked by a pair of 0-mV depolarizing pulses with an interval of 750 ms. (*A* and *B*) Representative traces for first and second EPSCs evoked by a pair of 0-mV depolarizing pulses with an interval of 750 ms. The durations of first preDPs were 3 ms (*A*, preDP3) or 30 ms (*B*, preDP30), and the second test pulse duration was 30 ms (DP30). EPSC traces were deconvolved to obtain quantal release rates (traces, second row). Cumulative release rates were calculated by integrating quantal release rates, and were fitted with biexponential functions to obtain the fast (blue and red solid lines) and slow components (broken lines). (*C*) Comparison of traces for second EPSCs (*Left*), quantal release rates (*Center*), and cumulative release (*Right*) evoked 750 ms after a preDP3 (blue) or after a preDP30 (red), using the same traces as shown in *A* and *B*. (*Inset*) Cumulative release scaled to the same peak. (Scale bar: 3 ms.)

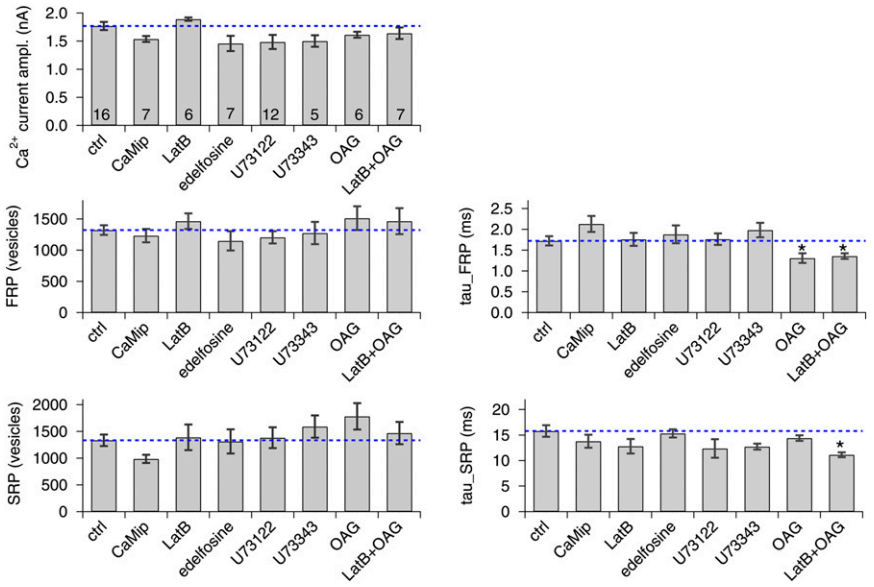

Fig. S2. Effects of drugs on the baseline estimates. Mean values for basal estimates for Ca^{2+} current amplitude (*Top*), FRP and SRP size (*Left*, *Middle*, and *Bottom*), and their release time constants τ (denoted by "tau_FRP" and "tau_SRP", respectively; *Right*).

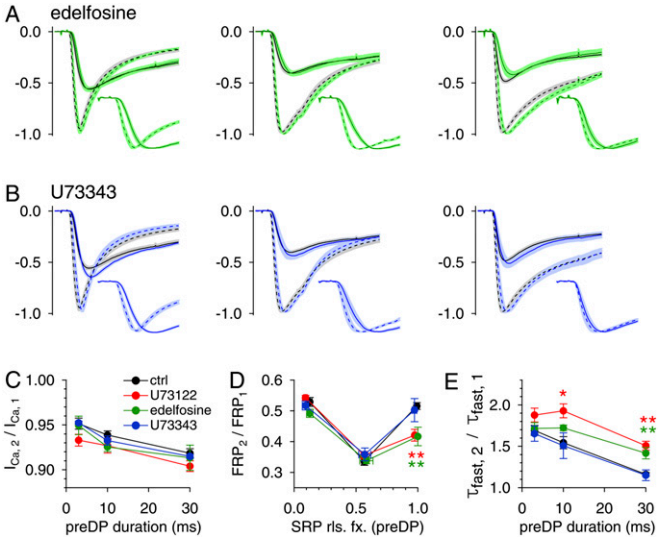

Fig. S3. Inhibition of phospholipase C retards superpriming of newly recruited FRP-SVs after a strong prepulse. (*A*) Averaged traces of $EPSC_1$ (broken line) and $EPSC_2$ (solid line) evoked by a dual pulse protocol (as shown in Fig. 1) with different preDPLs (*Left*, 3 ms; *Middle*, 10 ms; *Right*, 30 ms) in the presence of edelfosine (green). EPSCs were normalized to peak amplitude of the $EPSC_1$. $EPSC_1$ and $EPSC_2$ are superimposed. The SE range of averaged traces is depicted by shading of traces with a light color. (*B*) The same experiments as in *A* except for the presence of U73343 (inactive analogue of U73122, blue). Black traces in each panel represent the averaged EPSC traces evoked by the same pulse protocol in the absence of drugs. The image at the lower right of each panel shows an averaged trace of $EPSC_1$ and $EPSC_2$ scaled to the same peak for comparison of their time courses. (*C*) The ratio of the second to the first amplitude of presynaptic Ca^{2+} currents ($I_{Ca,2}/I_{Ca,1}$). Mean values are plotted as a function of preDPLs. (*D*) The recovered fraction of the FRP size at the second pulse (FRP_2/FRP_1) as a function of the fraction of SRP released by the first pulse. (*E*) Ratios of the release time constants (τ) of FRPs at the second pulse to those of FRPs at the first pulse ($\tau_{fast,2}/\tau_{fast,1}$) are plotted as a function of prepulse durations.

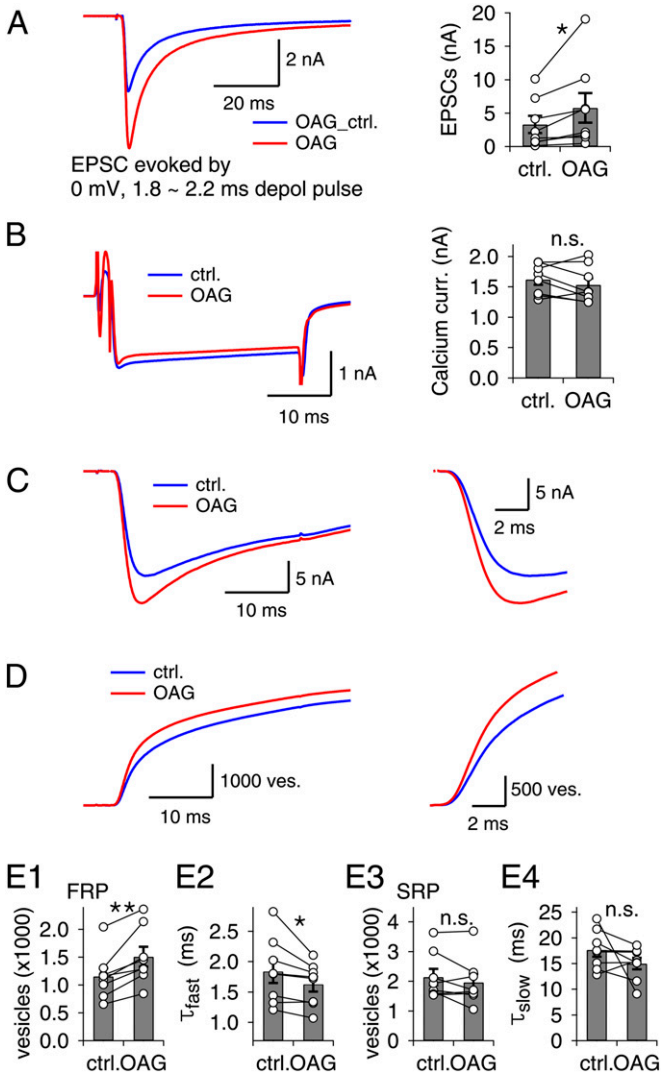

Fig. S4. Effects of OAG on the baseline fast and slow SV pool sizes and their release kinetics. (*A*) Averaged traces of EPSCs recorded before (blue) and after (red) bath application of 20 μM OAG. EPSCs were evoked by a presynaptic short depolarizing pulse (0 mV for 1.8–2.2 ms). Bar graph shows the mean values for EPSC amplitudes. OAG significantly enhanced the EPSC amplitude from 3.30 ± 1.28 nA to 5.79 ± 2.21 nA ($n = 8$; $P = 0.04$). (*B*) Averaged traces of Ca^{2+} currents evoked by DP30 and the mean amplitude values. (*C* and *D*) Averaged traces of corresponding EPSCs (*C*) and cumulative release curves (*D*) evoked by a DP30. (*Right*) Same traces on an expanded time scale. (*E*) Mean values for the FRP size (*1*), τ_{fast} (*2*), SRP size (*3*), and τ_{slow} (*4*). Circles connected with lines on the bar graphs indicate data from individual synapses. OAG significantly increased the FRP size from 1,156 ± 147 vesicles to 1,509 ± 178 vesicles ($n = 8$; $P = 0.002$), and accelerated τ_{fast} from 1.84 ± 0.19 ms to 1.69 ± 0.12 ms ($P = 0.04$). The parameters for SRP, however, were not altered by OAG. Values presented as mean ± SEM (*$P < 0.05$ and **$P < 0.01$, paired *t* test).

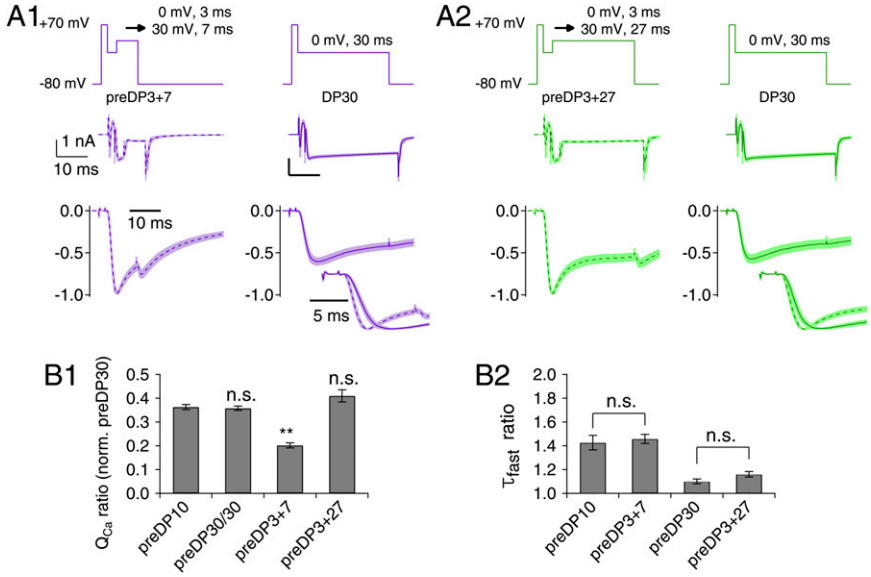

Fig. S5. Incomplete depletion of FRP is not responsible for the accelerated τ_{fast} recovery after a preDP30/30mV. (*A*) Two-step paired pulse protocol (*Top*) and resultant presynaptic Ca^{2+} currents (*Middle*) and EPSCs (*Bottom*). A preDP30/30mV (Fig. 6 *A*, *2*) may not completely deplete the FRP, and that remaining fast-releasing SVs may contribute to the recovery of τ_{fast}. To ensure the depletion of FRP, we applied a 3-ms depolarization step to 0 mV followed by a second 7-ms or 27-ms step to +30 mV as a preDP (denoted by preDP3+7 or preDP3+27). The upper rows of *1* and *2* show these pulse protocols, which are a step to 0 mV (first step) for 3 ms followed by a step to +30 mV (broken line) for 7 ms (*1*) or 27 ms (*2*). EPSCs were normalized to the peak amplitude of the $EPSC_1$. Images at lower right of each panel compare the time to peak of $EPSC_1$ (dotted line) and EPSC2 (solid line). The SE range of averaged traces is depicted by shading of the traces with a light color. (*B*) *1*, The ratio of total Ca^{2+} influx induced by a given prepulse protocol to that by a preDP30. *2*, Ratios of the $\tau_{fast,2}$ to $\tau_{fast,1}$ estimated under different prepulse protocols. The recovery of τ_{fast} after a preDP3+7 or a preDP3+27 was similar to that after a preDP10 or preDP30, respectively (preDP3+7, $n = 6$, $P = 0.40$; preDP3+27, $n = 5$, $P = 0.11$), showing that facilitation of superpriming critically depends on the duration of Ca^{2+} influx rather than on its magnitude. It should be noted that the τ_{fast} recovery was more facilitated by a preDP30/30mV or a preDP3+27 than by a preDP10 ($n = 6$; $P = 0.025$).

Table S1. Mean values for recovered FRP size and τ_{fast} after different prepulse protocols under control conditions or in the presence of U73122 or OAG

Prepulse protocol	Pulse duration, ms	Purpose	Ca^{2+} influx, % of preDP30	SRP depletion, %	Pool size recovery (FRP_2/FRP_1) at 750 ms, %			τ-Ratio ($\tau_{fast2}/\tau_{fast1}$) at 750 ms		
					Control	U73122	OAG	Control	U73122	OAG
preDP3	3	Deplete FRP while leaving SRP almost intact	11.5 ± 0.4	12.6 ± 1.9	52.9 ± 1.4	54.2 ± 0.8	48.6 ± 1.4	1.69 ± 0.06	1.88 ± 0.08	1.17 ± 0.0**
preDP10	10	Deplete FRP and SRP with low Ca influx	36.9 ± 0.4	56.7 ± 2.2	33.5 ± 1.3	35.5 ± 1.2	33.5 ± 2.1	1.54 ± 0.07	1.93 ± 0.08**	1.58 ± 0.15
preDP30/0mV (or preDP30)	30	Deplete both pools and provoke large long-lasting Ca influx	100	99.1 ± 0.6	51.6 ± 1.1	42.1 ± 1.9**	48.8 ± 1.7	1.16 ± 0.02	1.51 ± 0.05**	1.12 ± 0.05
preDP30/30mV	30	Similar to preDP30, provoking long-lasting but reduced Ca influx	35.8 ± 0.9	ND	42.0 ± 4.3	43.2 ± 2.3	ND	1.21 ± 0.04	1.78 ± 0.12**	ND
preDP3+7	10	Similar to preDP10, but provoking reduced Ca influx[a]	20.2 ± 1.1	36.1 ± 3.8	55.1 ± 3.0	ND	ND	1.46 ± 0.04	ND	ND
preDP3+27	30	Similar to preDP30/30mV, provoking long-lasting but reduced Ca influx[a]	41.0 ± 2.5	75.1 ± 2.1	51.5 ± 2.8	ND	ND	1.16 ± 0.02	ND	ND

Each protocol starts with a 2-ms episode at +70 mV to fully open Ca^{2+} channels followed by episodes to 0 mV (for maximum Ca^{2+} current) or +30 mV (for reduced Ca^{2+} current). ND, not determined. $^{**}P < 0.01$.

[a]The last two protocols include a 3-ms episode at 0 mV (maximum Ca^{2+} current) to guarantee full depletion of the FRP.